Robotica (2009) volume 27, pp. 1027–1038. © Cambridge University Press 2009
doi:10.1017/S026357470900544X

Teleoperation with kinematically redundant robot manipulators with sub-task objectives*

Nitendra Nath‡†, Enver Tatlicioglu§ and Darren M. Dawson‡

‡*Department of Electrical & Computer Engineering, Clemson University, Clemson, SC 29634-0915, USA*
§*Department of Electrical & Electronics Engineering, Izmir Institute of Technology, Gulbahce Koyu, Urla, Izmir 35430, Turkey*

(Received in Final Form: February 4, 2009. First published online: March 6, 2009)

SUMMARY
In this paper, control of nonlinear teleoperator systems where both the master and slave systems are kinematically redundant robot manipulators is addressed. The controller is developed under the assumption that the user and environmental input forces are unmeasurable. Lyapunov-based stability analysis is used to prove that the proposed controller yields asymptotic tracking results and ensures the coordination of the master and slave systems while satisfying a sub-task objective. Numerical simulation results are presented to illustrate the effectiveness of the proposed controller.

KEYWORDS: Teleoperation; Redundant manipulators; Control of robotic systems; Lyapunov-based control; Sub-control objectives.

1. Introduction

Teleoperation, where a human operator implements a task in a remote or hazardous environment, has been a mainstream research problem for a long time. Typically, a teleoperator system consists of a local site, where a user operates the master manipulator/system to drive the remotely located slave manipulator/system to implement a given task. Teleoperator systems have significant impact on some common applications including handling of hazardous materials, maneuvering mobile robots, underwater operations, and microsurgery.[2–5] Transparency,[6] keeping the human and the environment safe, proving the boundedness of closed-loop signals, and tracking a desired trajectory are important issues in teleoperation. The reader is referred to ref. [7] for a comprehensive overview of research and development in teleoperation over the last several years.

In several robotic applications, including teleoperation, the desired task is usually defined in the Cartesian coordinate frame attached to the robot manipulator's end-effector, which is commonly referred to as the *task-space*. When a robot manipulator has more degrees of freedom than required to implement a task in its task-space, it is called a kinematically redundant robot manipulator. The use of kinematically redundant robot manipulators usually complicates the control design; however, they provide greater flexibility to the end user to execute sophisticated or complicated tasks such as obstacle avoidance, grasping, and locomotion.[8] The fact, that the number of joints of a redundant robot manipulator is greater than the dimension of the task-space, results in joint motion in the null-space of the Jacobian matrix that does not affect the end-effector motion of the manipulator, generally known as *self-motion*. A user can deploy the self-motion for achieving a sub-task objective while the task-space controller achieves the primary task for a particular application. As noted in refs. [9–11], for redundant robots, given a desired task-space trajectory, an infinite number of inverse kinematic solutions exist that complicates the selection of a reasonable desired joint trajectory, to satisfy the control requirements as well as the sub-task objectives. The reader is referred to ref. [12] for different sub-task objectives and to refs. [9, 13–17], and the references therein, for some of the past research related to the controllers for redundant robot manipulators.

Teleoperation with kinematically redundant robot manipulators is an interesting open research area. Some past work that discusses teleoperation with kinematically redundant robot manipulators can be found in refs. [18, 19]. Hwang and Hannaford[18] described the performance of a teleoperator system where only the slave system was a redundant robot manipulator. This work failed to provide robustness when the robot operates close to its kinematic singularities or for high joint velocities. In ref. [18], the controller was developed for the primary task and the sub-task objectives were considered as an add-on to the tracking objective; hence, completion of certain sub-task objectives such as joint-limit avoidance was not guaranteed. Das *et al.*[19] developed kinematic controllers for redundant teleoperator system to avoid obstacle collision by utilizing visual display of the slave environment system where just the task-space control was applied. While addressing an interesting problem, refs. [18] and [19] failed to make complete use of the properties of the redundant manipulators.

This work aimed to develop a novel control scheme for teleoperator systems where master and slave systems are kinematically redundant robot manipulators. The control objectives are to track a desired task-space trajectory, to ensure the coordination between the master and the slave systems and to utilize the self-motion of the redundant robot manipulators to achieve sub-task objectives. The control problem is further complicated due to unmeasurable user and

* A preliminary version of this paper has appeared in ref. [1].
† Corresponding author. E-mail: nnath@clemson.edu

https://doi.org/10.1017/S026357470900544X Published online by Cambridge University Press

environmental input forces. To achieve the control objectives, first the dynamic models of the master and slave systems are put together to form a combined dynamic model for the teleoperator system. Then, robust integral of the sign of the error terms are utilized in the design of a force observer to estimate the unmeasurable input forces. Next, a null-space decomposition is utilized to divide the control input and the input forces into their task-space and null space components; thus, the control development is separated into two parts, namely task-space control and null-space control. To facilitate the task-space control development, an invertible transformation[20] is utilized to encode the control objectives. Another continuous nonlinear observer is designed to estimate the task-space component of the input forces. The task-space controller is developed to meet the task-space tracking objective and to ensure the coordination of the master and slave systems. In the design of the task-space desired trajectory, an optional strategy of encoding a velocity field assist mechanism[20] is provided to help the user in controlling the slave system. The null-space component of the controller is then designed to meet the null-space velocity tracking objective. Finally, a sub-task controller is developed to make use of the kinematic redundancy of the master and slave systems. Lyapunov-based techniques are utilized in the design of the controllers and the force observers. The performance of the proposed controller and the force observers is demonstrated by numerical simulation results where singularity avoidance is implemented as the sub-task objective.

The paper is organized as follows: in Section 2 the dynamic and kinematic models of a teleoperator system are presented. Section 3 deals with the force observer development that accounts for the unmeasurable forces. Section 4 describes the development for the task-space controller along with the observer designed to estimate the task-space component of the input forces and the stability analysis. Null-space and sub-task controller developments are presented in Sections 5 and 6, respectively. Section 7 presents numerical simulation results that demonstrate the efficiency of the proposed controller.

2. Dynamic and Kinematic Models

The dynamic model for a $2n$-DOF nonlinear teleoperator system consisting of a revolute n-DOF master and a revolute n-DOF slave system is described by the following expressions

$$M_1(\theta_1)\ddot{\theta}_1 + N_1(\theta_1, \dot{\theta}_1)\dot{\theta}_1 = T_1(t) + F_{\mathrm{H}}(t) \tag{1}$$

$$M_2(\theta_2)\ddot{\theta}_2 + N_2(\theta_2, \dot{\theta}_2)\dot{\theta}_2 = T_2(t) + F_{\mathrm{E}}(t) \tag{2}$$

where $\theta_i(t), \dot{\theta}_i(t), \ddot{\theta}_i(t) \in \mathbb{R}^n$ denote the joint-space position, velocity, and acceleration for the master and the slave systems, respectively, $M_i(\cdot)$, $N_i(\cdot) \in \mathbb{R}^{n\times n}$ represent the known inertia effects and other dynamic effects, respectively, $T_i(t) \in \mathbb{R}^n$ represents the control input vector where $i = 1$ denotes the master system and $i = 2$ denotes the slave system. In (1) and (2), $F_{\mathrm{H}}(t) \in \mathbb{R}^n$ represents the unmeasurable user input force applied to the master system, and $F_{\mathrm{E}}(t) \in \mathbb{R}^n$ represents the unmeasurable input force from the environment. The subsequent development utilizes the property that the inertia matrices are positive definite, symmetric and satisfy the following inequalities[21]:

$$m_{1i}\,\|\xi\|^2 \le \xi^T M_i(\cdot)\,\xi \le m_{2i}\,\|\xi\|^2 \tag{3}$$

$\forall \xi \in \mathbb{R}^n$ and $i = 1, 2$ where $m_{1i}, m_{2i} \in \mathbb{R}$ are positive constants, and $\|\cdot\|$ denotes the standard Euclidean norm.

Assumption 1. *To achieve the control objectives, the subsequent development is derived based on the assumption that $\theta_i(t)$, $\dot{\theta}_i(t)$ are measurable, and $M_i(\cdot)$, $N_i(\cdot)$ are second-order differentiable for $i = 1, 2$.*

Assumption 2. *The unmeasurable input forces and their first and second time derivatives, $F_H(t)$, $\dot{F}_H(t)$, $\ddot{F}_H(t)$, $F_E(t)$, $\dot{F}_E(t)$, and $\ddot{F}_E(t)$ are bounded (see refs. [22] and [23] for the precedence of this type of assumption).*

The kinematic models for the master and slave systems are described by the following expressions:

$$\dot{x}_m = J_1(\theta_1)\,\dot{\theta}_1 \tag{4}$$

$$\dot{x}_s = J_2(\theta_2)\,\dot{\theta}_2 \tag{5}$$

where $x_m(t)$, $x_s(t) \in \mathbb{R}^m$ are the task-space positions of the master and the slave systems, respectively, $\dot{x}_m(t)$, $\dot{x}_s(t) \in \mathbb{R}^m$ are the task-space velocities of the master and the slave systems, respectively, and $J_1(\theta_1)$, $J_2(\theta_2) \in \mathbb{R}^{m\times n}$ are the Jacobian matrices for the master and the slave systems, respectively. To facilitate the control development, $x(t) \in \mathbb{R}^{2m}$ and $\theta(t) \in \mathbb{R}^{2n}$ are defined as follows:

$$x \triangleq \begin{bmatrix} x_m^T & x_s^T \end{bmatrix}^T \tag{6}$$

$$\theta \triangleq \begin{bmatrix} \theta_1^T & \theta_2^T \end{bmatrix}^T. \tag{7}$$

After utilizing (4)–(7) the following expression can be obtained

$$\dot{x} = J(\theta)\,\dot{\theta} \tag{8}$$

where $J(\cdot) \in \mathbb{R}^{2m\times 2n}$ is defined as follows*:

$$J \triangleq \begin{bmatrix} J_1 & 0_{m\times n} \\ 0_{m\times n} & J_2 \end{bmatrix}. \tag{9}$$

To facilitate the subsequent development, the dynamic models of the teleoperator system given in (1) and (2) can be combined as follows:

$$M\ddot{\theta} + N\dot{\theta} = T + F \tag{10}$$

* Throughout the paper, $0_{i\times j}$ and I_i will be used to denote an $i \times j$ zero matrix and an $i \times i$ standard identity matrix, respectively.

https://doi.org/10.1017/S026357470900544X Published online by Cambridge University Press

where $M(\cdot), N(\cdot) \in \mathbb{R}^{2n\times 2n}$, $T(\cdot)$, and $F(\cdot) \in \mathbb{R}^{2n}$ are defined as follows:

$$M \triangleq \begin{bmatrix} M_1 & 0_{n\times n} \\ 0_{n\times n} & M_2 \end{bmatrix} \tag{11}$$

$$N \triangleq \begin{bmatrix} N_1 & 0_{n\times n} \\ 0_{n\times n} & N_2 \end{bmatrix} \tag{12}$$

$$T \triangleq \begin{bmatrix} T_1^T & T_2^T \end{bmatrix}^T \tag{13}$$

$$F \triangleq \begin{bmatrix} F_H^T & F_E^T \end{bmatrix}^T. \tag{14}$$

The kinematic model given in (8) can be written as follows:

$$\dot{x} = J_f \theta_f \tag{15}$$

where $\theta_f(t) \in \mathbb{R}^{2n}$ is defined as follows:

$$\theta_f \triangleq M\dot{\theta} \tag{16}$$

and $J_f(\theta) \in \mathbb{R}^{2m\times 2n}$ is a Jacobian-type matrix, defined as follows:

$$J_f \triangleq JM^{-1}. \tag{17}$$

The primary control design objective for teleoperator systems is to ensure the coordination between the master and the slave systems and to meet the tracking objective in the following sense:

$$x_s(t) \to x_m(t) \text{ as } t \to \infty \tag{18}$$

$$x_m(t) \to \xi_1(t) \text{ as } t \to \infty \tag{19}$$

where $\xi_1(t) \in \mathbb{R}^m$ is a subsequently designed desired trajectory. Other control objectives are to prove the boundedness of the closed-loop signals and accomplishment of a sub-task objective.

Remark 1. *The pseudo-inverse of the Jacobian $J_f(\theta)$ denoted by $J_f^+(\theta) \in \mathbb{R}^{2n\times 2m}$ is defined as follows:*

$$J_f^+ \triangleq J_f^T \left(J_f J_f^T\right)^{-1} \tag{20}$$

where $J_f^+(\theta)$ satisfies the following equality:

$$J_f J_f^+ = I_{2m}. \tag{21}$$

As shown in ref. [9], the pseudo-inverse defined by (20) satisfies the following Moore–Penrose conditions:

$$J_f J_f^+ J_f = J_f \qquad J_f^+ J_f J_f^+ = J_f^+$$
$$(J_f^+ J_f)^T = J_f^+ J_f \qquad (J_f J_f^+)^T = J_f J_f^+. \tag{22}$$

Additionally, the matrix $(I_{2n} - J_f^+ J_f)$ satisfies the following properties:

$$(I_{2n} - J_f^+ J_f)(I_{2n} - J_f^+ J_f) = I_{2n} - J_f^+ J_f \tag{23}$$

$$(I_{2n} - J_f^+ J_f)^T = I_{2n} - J_f^+ J_f \tag{24}$$

$$J_f(I_{2n} - J_f^+ J_f) = 0_{2m\times 2n} \tag{25}$$

$$(I_{2n} - J_f^+ J_f)J_f^+ = 0_{2n\times 2m} \tag{26}$$

$$(I_{2n} - J_f^+ J_f)J_\phi = J_\phi \tag{27}$$

where $J_\phi(t) \in \mathbb{R}^{2n\times 2n}$ is defined as follows[*]*:*

$$J_\phi \triangleq \dot{J}_f^+ J_f + J_f^+ \dot{J}_f J_f^+ J_f. \tag{28}$$

Remark 2. *During the control development, it is assumed that the minimum singular value of the manipulator Jacobian matrix, denoted by σ_m, is greater than a known small positive constant $\delta > 0$, such that $\max\{\|J_f^+(\theta)\|\}$ is known a priori and all kinematic singularities are always avoided.*[24–28]

3. Force Observer Development

In this section, a nonlinear force observer is designed to compensate for the unmeasurable user and environmental forces.

3.1. Closed-loop error system

Taking the time derivative of (16) results in the following expression:

$$\dot{\theta}_f = \dot{M}\dot{\theta} + T + F - N\dot{\theta} \tag{29}$$

where (10) was utilized. Based on the assumption of the exact model knowledge, the control input is designed as follows:

$$T \triangleq u + (N - \dot{M})\dot{\theta} \tag{30}$$

where $u(t) \in \mathbb{R}^{2n}$ is a subsequently designed auxiliary control input. After substituting (30) into (29), the following simplified expression can be obtained:

$$\dot{\theta}_f = u + F. \tag{31}$$

The estimate of (31) is defined as follows:

$$\dot{\hat{\theta}}_f \triangleq u + \hat{F} \tag{32}$$

where $\hat{F}(t) \in \mathbb{R}^{2n}$ is the estimate of $F(t)$ which is to be designed, $\hat{\theta}_f(t)$ is the estimate of $\theta_f(t)$, and $\dot{\hat{\theta}}_f$ is the estimate of $\dot{\theta}_f(t)$. To facilitate the development of the closed-loop error system, the observer error, denoted by $\tilde{\theta}_f(t) \in \mathbb{R}^{2n}$, is defined as follows:

$$\tilde{\theta}_f \triangleq \hat{\theta}_f - \theta_f. \tag{33}$$

[*] The reader is referred to Appendix B for the proof of (27).

https://doi.org/10.1017/S026357470900544X Published online by Cambridge University Press

After taking the time derivative of (33), the following expression can be obtained:

$$\dot{\tilde{\theta}}_f = \dot{\hat{F}} - \dot{F} \tag{34}$$

where (31) and (32) were utilized. A filtered observer error signal, denoted by $r_f(t) \in \mathbb{R}^{2n}$, is defined as follows:

$$r_f \triangleq \dot{\tilde{\theta}}_f + \tilde{\theta}_f. \tag{35}$$

The error system dynamics for $r_f(t)$ can be derived by taking time derivative of (35)

$$\dot{r}_f = \ddot{\hat{F}} - \dot{F} + r_f - \tilde{\theta}_f \tag{36}$$

where the time derivatives of (34) and (35) were utilized. Based on the subsequent stability analysis, the proportional-integral like nonlinear observer $\hat{F}(t)$ is designed as follows:

$$\dot{\hat{F}} \triangleq -(K_s + 1)\left[\tilde{\theta}_f(t) - \tilde{\theta}_f(t_0) + \int_{t_0}^{t} \tilde{\theta}_f(\tau)\,\mathrm{d}\tau\right] - (\beta_1 + \beta_2)\int_{t_0}^{t} \mathrm{sgn}(\tilde{\theta}_f(\tau))\,\mathrm{d}\tau \tag{37}$$

where $K_s, \beta_1, \beta_2 \in \mathbb{R}$ are positive control gains, and $\mathrm{sgn}(\cdot)$ denotes the vector signum function applied to each element of $\tilde{\theta}_f(t)$. In (37), the term $\tilde{\theta}_f(t_0)$ is used to ensure that $\hat{F}(t_0) = 0_{2n\times 1}$. The time derivative of (37) is obtained as follows:

$$\ddot{\hat{F}} = -(K_s + 1)r_f - (\beta_1 + \beta_2)\mathrm{sgn}(\tilde{\theta}_f) \tag{38}$$

where (35) was utilized. Substituting (38) into (36) results in the following closed-loop error system:

$$\dot{r}_f = -K_s r_f - (\beta_1 + \beta_2)sgn(\tilde{\theta}_f) - \dot{F} - \tilde{\theta}_f. \tag{39}$$

Remark 3. *After utilizing (14) and Assumption 2, $\|\dot{F}(t)\|$ and $\|\ddot{F}(t)\|$ can be upper bounded as follows:*

$$\|\dot{F}(t)\| \le \varsigma_1 \qquad \|\ddot{F}(t)\| \le \varsigma_2 \tag{40}$$

where $\varsigma_1, \varsigma_2 \in \mathbb{R}$ represent positive bounding constants.

3.2. Stability analysis

Theorem 1. *The observer given in (37) guarantees that all signals are bounded and $\hat{F}(t) \to F(t)$ as $t \to \infty$ provided the control gain β_1, introduced in (37), is selected to satisfy the following sufficient condition:*

$$\beta_1 > \varsigma_1 + \varsigma_2 \tag{41}$$

where ς_1 and ς_2 were introduced in (40).

Proof. See Theorem 5 in ref. [12] for a similar proof.

4. Task-Space Controller Development

To facilitate the task-space control development, an invertible transformation that encodes the control objectives is defined as follows*:

$$\bar{x} \triangleq Sx + \begin{bmatrix} 0_{m\times 1} \\ \xi_2 \end{bmatrix} \tag{42}$$

where $\xi_2(t) \in \mathbb{R}^m$ is an auxiliary signal that will be designed subsequently, $\bar{x} \in \mathbb{R}^{2m}$, and $S \in \mathbb{R}^{2m\times 2m}$ is defined as follows:

$$S \triangleq \begin{bmatrix} I_m & 0_{m\times m} \\ I_m & -I_m \end{bmatrix}. \tag{43}$$

To meet the control objectives, a filtered tracking error signal, denoted by $r_T(t) \in \mathbb{R}^{2m}$, is defined as follows:

$$r_T \triangleq \dot{s}_T + s_T \tag{44}$$

where $s_T(t) \in \mathbb{R}^{2m}$ is defined as follows:

$$s_T \triangleq \dot{e}_T + e_T \tag{45}$$

where $e_T(t) \in \mathbb{R}^{2m}$ is defined as follows:

$$e_T \triangleq \xi_d - \bar{x}. \tag{46}$$

where $\xi_d(t) \in \mathbb{R}^{2m}$ is defined as follows:

$$\xi_d \triangleq \begin{bmatrix} \xi_1^T & \xi_2^T \end{bmatrix}^T \tag{47}$$

where $\xi_1(t) \in \mathbb{R}^m$ is the actual desired trajectory that will be tracked by the master and the slave systems. After utilizing (6), (42), and (47), the error signal $e_T(t)$ can be written as follows:

$$e_T \triangleq \begin{bmatrix} e_1 \\ e_2 \end{bmatrix} = \begin{bmatrix} \xi_1 - x_m \\ x_s - x_m \end{bmatrix} \tag{48}$$

where $e_1(t) \in \mathbb{R}^m$ represents the tracking error between the master system and the desired trajectory $\xi_1(t)$, and $e_2(t) \in \mathbb{R}^m$ represents the coordination error between the master and the slave systems. From (48), it is clear that if $\|e_T(t)\| \to 0$ then $x_s(t) \to x_m(t)$ and $x_m(t) \to \xi_1(t)$.

Remark 4. *The input force defined in (14) is decomposed** *as follows:*

$$F \triangleq J_f^+ F_T + (I_{2n} - J_f^+ J_f)F_N \tag{49}$$

where $F_T(t) \in \mathbb{R}^{2m}$ and $F_N(t) \in \mathbb{R}^{2n}$ are the task-space and the null-space components of the unmeasurable input forces.

* The reader is referred to ref. [20] for a detailed explanation of the transformation.

* In redundant robot control the control development is usually done in two subsections,[24–29] namely, the task-space control and the null-space control; thus, the input forces affecting the system is decomposed into its components where the null-space forces results in null-space motion (see [30]).

https://doi.org/10.1017/S026357470900544X Published online by Cambridge University Press

The auxiliary control input, $u(t)$ is designed as follows:

$$u \triangleq J_f^+ u_T + (I_{2n} - J_f^+ J_f) u_N \tag{50}$$

where $u_T(t) \in \mathbb{R}^{2m}$ and $u_N(t) \in \mathbb{R}^{2n}$ represent subsequently designed task-space and null-space components of the auxiliary control input, respectively.

To compensate for the task-space component of the unmeasurable input forces, a nonlinear force observer is designed subsequently which is also utilized to drive the target system. The desired trajectory $\xi_d(t)$ is generated by the following second-order coupled dynamic target system[20]:

$$\dot{\xi}_d = \gamma \begin{bmatrix} \varphi(\xi_1) \\ 0_{m\times 1} \end{bmatrix} + \eta_d \tag{51}$$

$$\dot{\eta}_d + B_T \eta_d + C_T \lambda_d = \hat{F}_T \tag{52}$$

where $\eta_d(t) \in \mathbb{R}^{2m}$ is an auxiliary filter signal, B_T, $C_T \in \mathbb{R}^{2m\times 2m}$ represent constant, positive definite, diagonal matrices, $\hat{F}_T(t) \in \mathbb{R}^{2m}$ is a subsequently designed nonlinear observer to estimate $F_T(t)$, $\varphi(\cdot) \in \mathbb{R}^m$ is a velocity field function[31] that encodes the user assist mechanism, and γ is a constant gain that is either 0 or 1. It should be noted that, when $\gamma = 1$, the user assist mechanism is enabled and it is disabled when $\gamma = 0$. Also, in (52) the term $\lambda_d(t) \in \mathbb{R}^{2m}$ is defined as follows:

$$\lambda_d \triangleq \xi_d - \gamma \begin{bmatrix} \int_{t_0}^{t} \varphi(\xi_1(\tau))\, \mathrm{d}\tau \\ 0_{m\times 1} \end{bmatrix}. \tag{53}$$

It is worthwhile to mention that when the user-assist mechanism is disabled ($\gamma = 0$), the target system defined by (51) and (52) becomes a standard impedance model.

Remark 5. *The velocity field function $\varphi(\cdot)$ is assumed to be designed such that, from (51), if $\eta_d(t) \in \mathcal{L}_\infty$ then $\xi_d(t)$, $\dot{\xi}_d(t) \in \mathcal{L}_\infty$. Subsequent analysis shows that $\hat{F}_T(t) \in \mathcal{L}_\infty$. These facts can be utilized along with the analysis in Appendix G of ref. [12] to prove that all the signals in the dynamic target system along with their higher order derivatives are bounded.*

4.1. Closed-loop error system

Taking the time derivative of (15) results in the following expression:

$$\ddot{x} = u_T + F_T + \dot{J}_f \theta_f \tag{54}$$

where (21), (25), (31), (49), and (50) were utilized. After taking the second time derivative of (42), the following expression is obtained:

$$\dddot{x} = S(u_T + \dot{J}_f \theta_f) + \dot{\bar{F}}_T + \begin{bmatrix} 0_{m\times 1} \\ \dddot{\xi}_2 \end{bmatrix} \tag{55}$$

where (54) was utilized and $\bar{F}_T(t) \in \mathbb{R}^{2m}$ is defined as follows:

$$\bar{F}_T \triangleq S F_T. \tag{56}$$

To facilitate the closed-loop error system for $r_T(t)$, the error system dynamics for $s_T(t)$ and $e_T(t)$ are derived first. After taking the second-order derivative of (46), the following expression is obtained

$$\ddot{e}_T = \gamma \begin{bmatrix} \dot{\varphi}(\xi_1) \\ 0_{m\times 1} \end{bmatrix} + \dot{\hat{F}}_T - B_T \dot{\eta}_d - C_T \dot{\lambda}_d - S(\dot{u}_T + \ddot{J}_f \theta_f) - \dot{\bar{F}}_T - \begin{bmatrix} 0_{m\times 1} \\ \dddot{\xi}_2 \end{bmatrix} \tag{57}$$

where (51), (52), and (55) were utilized. The task-space component of the auxiliary control input $u_T(t)$ is designed as follows:

$$u_T \triangleq -\dot{J}_f \theta_f + S^{-1} \left\{ \gamma \begin{bmatrix} \dot{\varphi}(\xi_1) \\ 0_{m\times 1} \end{bmatrix} - B_T \eta_d - C_T \lambda_d - \begin{bmatrix} 0_{m\times 1} \\ \ddot{\xi}_2 \end{bmatrix} \right\} + S^{-1} \bar{u}_T \tag{58}$$

where $\bar{u}_T(t) \in \mathbb{R}^{2m}$ is a subsequently designed auxiliary control input. After substituting (58) into (57), the following simplified expression is obtained:

$$\ddot{e}_T = \dot{\hat{F}}_T - \dot{\bar{F}}_T - \dot{\bar{u}}_T. \tag{59}$$

The time derivative of $s_T(t)$ can be obtained as follows:

$$\dot{s}_T = \dot{\hat{F}}_T - \dot{\bar{F}}_T - \dot{\bar{u}}_T + s_T - e_T \tag{60}$$

where (45) and (59) were utilized. Based on (60), the auxiliary control input $\bar{u}_T(t)$ is designed as follows:

$$\dot{\bar{u}}_T \triangleq s_T - e_T. \tag{61}$$

After substituting (61) into (60), the following simplified expression is obtained:

$$\dot{s}_T = \dot{\hat{F}}_T - \dot{\bar{F}}_T. \tag{62}$$

The error system dynamics for $r_T(t)$ can be derived by taking the time derivative of (44)

$$\dot{r}_T = \dot{\hat{F}}_T - \dot{\bar{F}}_T + r_T - s_T \tag{63}$$

where (44) and the time derivative of (62) were utilized. Based on (63), the proportional-integral like nonlinear observer introduced in (52) is designed as follows:

$$\dot{\hat{F}}_T \triangleq -(K_T + 1)\left[s_T(t) - s_T(t_0) + \int_{t_0}^{t} s_T(\tau)\, \mathrm{d}\tau \right] - (\beta_3 + \beta_4) \int_{t_0}^{t} \mathrm{sgn}(s_T(\tau))\, \mathrm{d}\tau \tag{64}$$

where K_T, β_3, $\beta_4 \in \mathbb{R}$ are positive control gains. In (64), the term $s_T(t_0)$ ensures that $\hat{F}_T(t_0) = 0_{2m\times 1}$. The time derivative

https://doi.org/10.1017/S026357470900544X Published online by Cambridge University Press

of (64) is obtained as follows:

$$\dot{\hat{F}}_T = -(K_T + 1)r_T - (\beta_3 + \beta_4)\,\mathrm{sgn}(s_T) \tag{65}$$

where (44) was utilized. After substituting (65) into (63), the following closed-loop error system is obtained:

$$\dot{r}_T = -K_T r_T - (\beta_3 + \beta_4)\,\mathrm{sgn}(s_T) - \dot{\tilde{F}}_T - s_T. \tag{66}$$

Remark 6. *After utilizing (14), Assumption 2, (49), and (56), $\|\dot{\tilde{F}}_T(t)\|$ and $\|\ddot{\tilde{F}}_T(t)\|$ can be upper bounded as follows:*

$$\|\dot{\tilde{F}}_T(t)\| \le \varsigma_3 \qquad \|\ddot{\tilde{F}}_T(t)\| \le \varsigma_4 \tag{67}$$

where ς_3, $\varsigma_4 \in \mathbb{R}$ represent positive bounding constants.

4.2. Stability analysis

Theorem 2. *The controller given in (58) and (61) and the observer in (64) guarantee that all signals are bounded under the closed-loop operation and that coordination between the master and the slave systems, and the tracking objective are met in the sense that*

$$x_s(t) \to x_m(t) \ \text{as}\ t \to \infty \tag{68}$$

$$x_m(t) \to \xi_1(t) \ \text{as}\ t \to \infty \tag{69}$$

provided the control gain β_3 is selected to satisfy the sufficient condition

$$\beta_3 > \varsigma_3 + \varsigma_4. \tag{70}$$

Proof. See Theorem 5 in ref. [12] for a similar proof.

5. Null-Space Controller Development

In this section, the null-space controller $u_N(t)$ will be designed to meet the null-space velocity tracking objective. In the controller design, the redundancy of the master and the slave manipulators will be utilized to perform certain sub-task objectives required for a particular application. To integrate this sub-task objective into the controller, an auxiliary control signal, denoted by $g(t)$, will be introduced. This auxiliary controller is designed through the joint motion in the null-space of the Jacobian matrix.

The null-space velocity tracking error, denoted by $\dot{e}_N(t) \in \mathbb{R}^{2n}$, is defined as[32]

$$\dot{e}_N \triangleq (I_{2n} - J_f^+ J_f)(g - \theta_f) \tag{71}$$

where $g(t) \in \mathbb{R}^{2n}$ is the subsequently designed sub-task controller. After utilizing (31), (49), and (50) the following expression is obtained:

$$\dot{\theta}_f = J_f^+ u_T + J_f^+ F_T + (I_{2n} - J_f^+ J_f)(u_N + F_N). \tag{72}$$

After taking the time derivative of (71), the dynamics of $\dot{e}_N(t)$ can be obtained as follows:

$$\ddot{e}_N = (I_{2n} - J_f^+ J_f)\dot{g} - (\dot{J}_f^+ J_f + J_f^+ \dot{J}_f)(g - \theta_f) - (I_{2n} - J_f^+ J_f)(u_N + F_N) \tag{73}$$

where (21), (23), (26), (71), and (72) were utilized. After adding and subtracting the term $J_f^+ \dot{J}_f J_f^+ J_f (g - \theta_f)$ to the right-hand side of (73), the following expression is obtained:

$$\ddot{e}_N = (I_{2n} - J_f^+ J_f)(\dot{g} - u_N) + J_f^+ F_T - F - J_\phi(g - \theta_f) - J_f^+ \dot{J}_f \dot{e}_N \tag{74}$$

where (28), (49), and (71) were utilized. The null-space component of the control input, $u_N(t)$ introduced in (50), is now designed as follows:

$$u_N \triangleq -J_\phi(g - \theta_f) + \dot{g} + K_N \dot{e}_N - \hat{F} \tag{75}$$

where $K_N \in \mathbb{R}$ is a positive constant. After substituting (75) into (74) and utilizing (21)–(27) the following expression is obtained:

$$\ddot{e}_N = -(I_{2n} - J_f^+ J_f)(K_N \dot{e}_N - \hat{F}) + J_f^+ F_T - F - J_f^+ \dot{J}_f \dot{e}_N. \tag{76}$$

Theorem 3. *The null-space component of the control input described by (75) guarantees that the null-space velocity tracking is obtained in the sense that $\|\dot{e}_N(t)\| \to 0$ as $t \to \infty$.*

Proof: See Appendix A.

6. Sub-Task Controller Development

In this section, the sub-task controller $g(t)$ is developed. The subsequent stability analysis shows that the sub-task objective is met if the Jacobian-related null-space matrix maintains full rank.

An auxiliary positive function $y_{ai}(t) \in \mathbb{R}$ is defined as follows:

$$y_{ai} \triangleq \exp(-k_i \rho_i(\theta_i)) \tag{77}$$

where $i = 1$ and 2 for the master and the slave systems, respectively, and $k_i \in \mathbb{R}$ is a positive constant, $\rho_i(\cdot) \in \mathbb{R}$ is a nonnegative function that is specific to a sub-task, and $\exp(\cdot)$ is the natural logarithmic exponential function. To facilitate the sub-task controller development, a positive function $y_a(t) \in \mathbb{R}$ is defined as follows:

$$y_a \triangleq y_{a1} + y_{a2}. \tag{78}$$

After taking the time derivative of (78), the following expression can be obtained:

$$\dot{y}_a = J_s \dot{\theta} \tag{79}$$

https://doi.org/10.1017/S026357470900544X Published online by Cambridge University Press

where (7) was utilized and $J_s(t) \in \mathbb{R}^{1\times 2n}$ is a Jacobian-type vector defined as follows:

$$J_s \triangleq \left[\frac{\partial y_{a1}}{\partial \theta_1} \quad \frac{\partial y_{a2}}{\partial \theta_2}\right]. \tag{80}$$

After utilizing (16), (79) can be expressed as follows:

$$\dot{y}_a = \bar{J}_s \theta_f \tag{81}$$

where the term $\bar{J}_s \triangleq J_s M^{-1} \in \mathbb{R}^{1\times 2n}$ is again a Jacobian-type vector. After adding and subtracting the term $\bar{J}_s(I_{2n} - J_f^+ J_f)(g - \theta_f)$ to the right-hand side of (81) the following simplified expression is obtained:

$$\dot{y}_a = \bar{J}_s(I_{2n} - J_f^+ J_f)g - \bar{J}_s J_f^+ J_f \theta_f - \bar{J}_s \dot{e}_N \tag{82}$$

where (71) was utilized. Based on the subsequent stability analysis, the sub-task controller is designed as follows:

$$g \triangleq -K_g \bar{J}_s^T y_a \tag{83}$$

where $K_g \in \mathbb{R}$ is a positive constant. After substituting (83) into (82), the following expression is obtained:

$$\dot{y}_a = -K_g \bar{J}_s(I_{2n} - J_f^+ J_f)\bar{J}_s^T y_a - \bar{J}_s J_f^+ J_f \theta_f - \bar{J}_s \dot{e}_N. \tag{84}$$

Theorem 4. *The control law described by (83) guarantees that $y_a(t)$ is ultimately bounded in the following sense:*

$$|y_a(t)| \leq \sqrt{\left|y_a^2(t_0)\right| \exp(-2\nu t) + \frac{\varepsilon}{\nu}} \tag{85}$$

provided that

$$K_g > \frac{1}{\bar{\delta}} \tag{86}$$

where ε, ν, $\bar{\delta} \in \mathbb{R}$ are positive constants.

Proof. See Theorem 2 in ref. [12] for a similar proof.

7. Simulation Results

A numerical simulation study was conducted to evaluate the performance of the proposed task-space and sub-task controllers using Mathworks Simulink program. A planar, three-joint, revolute robot dynamic model was considered for both the master and the slave systems[33] where the entries of $M_i(\cdot)$ and $N_i(\cdot)$ have the following forms*:

$$m_{i11} = p_1 + 2p_4 c_{i2} + 2p_5 c_{i23} + 2p_6 c_{i3} \quad m_{i22} = p_2 + 2p_6 c_{i3}$$
$$m_{i12} = p_2 + p_4 c_{i2} + p_5 c_{i23} + 2p_6 c_{i3} \quad m_{i23} = p_2 + p_6 c_{i3}$$
$$m_{i13} = p_2 + p_5 c_{i23} + p_6 c_{i3} \quad m_{i33} = p_3$$

$$n_{i11} = -p_4 s_{i2}\dot{\theta}_{i2} - p_5 s_{i23}\dot{\theta}_{i2} - p_5 s_{i23}\dot{\theta}_{i3} - p_6 s_{i3}\dot{\theta}_{i3}$$
$$n_{i12} = -(p_4 s_{i2} + p_5 s_{i23})(\dot{\theta}_{i1} + \dot{\theta}_{i2}) - p_5 s_{i23}\dot{\theta}_{i3} - 2p_6 s_{i3}\dot{\theta}_{i3}$$
$$n_{i13} = -(p_5 s_{i23} + p_6 s_{i3})(\dot{\theta}_{i1} + \dot{\theta}_{i3}) - p_5 s_{i23}\dot{\theta}_{i2}$$
$$n_{i21} = (p_4 s_{i2} + p_5 s_{i23})\dot{\theta}_{i1}$$
$$n_{i22} = -p_6 s_{i3}\dot{\theta}_{i3}$$
$$n_{i23} = -p_6 s_{i3}(2\dot{\theta}_{i1} + \dot{\theta}_{i2} + \dot{\theta}_{i3})$$
$$n_{i31} = (p_5 s_{i23} + p_6 s_{i3})\dot{\theta}_{i1}$$
$$n_{i32} = p_6 s_{i3}(2\dot{\theta}_{i1} + \dot{\theta}_{i2})$$
$$n_{i33} = 0$$

where $M_i(\cdot) = (m_{i,j,k})_{3\times 3}$ and $N_i(\cdot) = (n_{i,j,k})_{3\times 3}$ with $i = 1$ and 2 for the master and the slave systems, respectively, and the parameter $p_z \; \forall z = 1, \ldots, 6$ has the following values $p_1 = 1.2745\,[\mathrm{kg\,m^2}]$, $p_2 = 0.3946\,[\mathrm{kg\,m^2}]$, $p_3 = 0.0512\,[\mathrm{kg\,m^2}]$, $p_4 = 0.4752\,[\mathrm{kg\,m^2}]$, $p_5 = 0.1280\,[\mathrm{kg\,m^2}]$, and $p_6 = 0.1152\,[\mathrm{kg\,m^2}]$.

Since most real robot manipulators are required to avoid the configurations that result in singularities that tend to decrease the manipulability of the robot manipulator, singularity avoidance is considered as an interesting sub-task control objective. The objective of this sub-task is to keep the configurations of the master and the slave systems in such a way that neither of the systems reaches its singular position.* For this particular sub-task, the auxiliary signal $\rho_i(\theta_i)$ is defined as the manipulability measure and is expressed by the following expression[12]:

$$\rho_i = \sqrt{\det\left[J_i J_i^T\right]} \quad \forall i = 1, 2 \tag{87}$$

where det[·] is the determinant of the Jacobian matrix for $i = 1$ and 2 for the master and the slave systems, respectively. It should be noted that when the robot is in a singular configuration, $\rho_i(\cdot) = 0$. For this sub-task objective, the problem is set up to satisfy $\rho_i(\cdot) > 0 \, \forall i = 1, 2$ which can be achieved by keeping $y_{ai}(t) < 1 \forall i = 1, 2$ or as seen from (78), $y_a(t) < 2$. Based on Theorem 4, it is clear that $y_a(t) < 2$ if the following inequality holds:

$$\sqrt{|y_a^2(t_0)| + \frac{\varepsilon}{\nu}} < 2 \tag{88}$$

which can be achieved by proper selection of the initial conditions of the robot manipulators, control gains K_g, k_1, k_2, and bounding constants. From (77), (85), (87), and (88), it can be clearly seen that $\rho_i(\cdot) > 0 \quad \forall i = 1, 2 \quad \forall t$, provided the sufficient condition (86) is met; thus, guaranteeing that both master and slave systems avoid singular configurations.

* The notations c_{ij}, c_{ijk}, c_{ijkn}, s_{ij}, s_{ijk}, and s_{ijkn} represent $\cos(\theta_{ij})$, $\cos(\theta_{ij} + \theta_{ik})$, $\cos(\theta_{ij} + \theta_{ik} + \theta_{in})$, $\sin(\theta_{ij})$, $\sin(\theta_{ij} + \theta_{ik})$, and $\sin(\theta_{ij} + \theta_{ik} + \theta_{in}) \; \forall j, k, n$, respectively, where $i = 1$ denotes the master system and $i = 2$ denotes the slave system.

* It should be noted that Remark 2 is essential for the development and it is a standard assumption in redundant robot control literature[24–28] whereas, the singularity avoidance sub-task guarantees that all singularities are avoided for all practical purposes.

https://doi.org/10.1017/S026357470900544X Published online by Cambridge University Press

The user and environmental input forces were set equal to the following time-varying signals:

$$F_H = \begin{bmatrix} -\sin(2t) - 0.18\dot{x}_{s1} - 0.3x_{s1} \\ -\cos(2t) - 0.18\dot{x}_{s2} - 0.3x_{s2} \\ 0 \end{bmatrix}$$

$$F_E = \begin{bmatrix} 0.18\dot{x}_{s1} + 0.3x_{s1} \\ 0.18\dot{x}_{s2} + 0.3x_{s2} \\ 0 \end{bmatrix}$$

where the environmental force vector $F_E(t)$ was set to be a spring and linear damping-like force vector and $x_{s1}(t)$, $x_{s2}(t) \in \mathbb{R}$ are the scalar Euclidean coordinates of the slave system. The forward kinematics for the end-effector of a planar three-joint robot manipulator[12] was utilized for the master and the slave systems in the simulation with link lengths as $l_1 = 0.40$ [m], $l_2 = 0.36$ [m], $l_3 = 0.32$ [m] for both the master and the slave systems. The target system, described by (51) and (52), is simplified as follows:

$$\dot{\xi}_1 = \gamma\varphi(\xi_1) + \eta_d \tag{89}$$

$$\dot{\eta}_d = \hat{F}_T. \tag{90}$$

The following planar task-space velocity field function was utilized[34]:

$$\varphi(\xi_1) = -2K(\xi_1)f(\xi_1)\begin{bmatrix}\xi_{1x}\\ \xi_{1y}\end{bmatrix} + 2c(\xi_1)\begin{bmatrix}-\xi_{1y}\\ \xi_{1x}\end{bmatrix}$$

where $\xi_1 = [\xi_{1x} \quad \xi_{1y}]^T$ is the desired end-effector position, and $f(\cdot)$, $K(\cdot)$, $c(\cdot) \in \mathbb{R}$ are defined as follows:

$$f(\xi_1) = \xi_{1x}^2 + \xi_{1y}^2 - r_0^2$$

$$K(\xi_1) = k_0\left(\sqrt{f^2(\xi_1)}\left\|\frac{\partial f(\xi_1)}{\partial \xi_1}\right\| + \epsilon\right)^{-1}$$

$$c(\xi_1) = \frac{c_0 \exp(-\mu\sqrt{f^2(\xi_1)})}{\left\|\frac{\partial f(\xi_1)}{\partial \xi_1}\right\|}. \tag{91}$$

In (91), $r_0 = 1$[m], $k_0 = 1\,[\mathrm{m\,s^{-1}}]$, $\epsilon = 0.005\,[\mathrm{m^3}]$, $c_0 = 1[\mathrm{m\,s^{-1}}]$, and $\mu = 1\,[\mathrm{m^{-1}}]$ were selected. The control gains were tuned based on trial and error approach, and were selected as follows:

$$K_s = 100 \qquad \beta_1 + \beta_2 = 50$$

$$K_T = 50 \qquad \beta_3 + \beta_4 = 10$$

$$K_g = 70,\ K_N = 50,\ k_1 = 1,\ k_2 = 1.$$

The master and the slave systems were set to be initially at rest with the following joint configurations*:

$$\theta_1(t_0) = [0.5 \quad 0.0 \quad 3.0]^T \qquad \text{[rad]}$$

$$\theta_2(t_0) = [0.5 \quad 0.1 \quad 0.0]^T \qquad \text{[rad]}.$$

* The initial joint configurations (in degrees) in the simulation study were chosen as [28.6, 0, 171] for the master system and [28.6, 5.7, 0] for the slave system. It is clear that both of these configurations are very close to the workspace-interior singularities[35] [28.6, 0, 180] and [28.6, 0, 0], respectively.

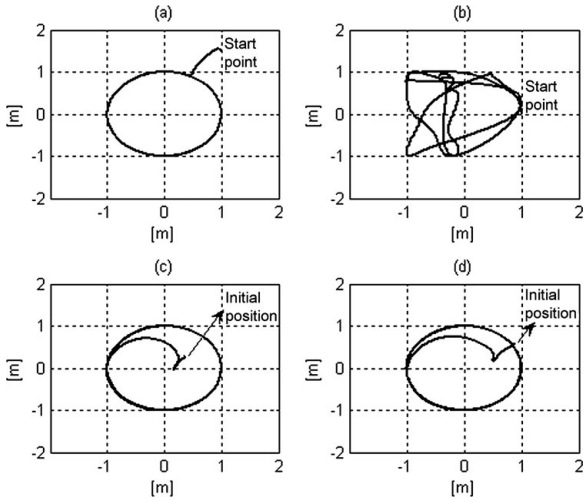


Fig. 1. End-effector positions: (a) desired end-effector position $\xi_1(t)$ with user assistance (when $\gamma = 1$); (b) desired end-effector position $\xi_1(t)$ without user assistance (when $\gamma = 0$); (c) end-effector position of the master system $x_m(t)$ with user assistance (when $\gamma = 1$); (d) end-effector position of the slave system $x_s(t)$ with user assistance (when $\gamma = 1$).

The initial configuration of the master and slave systems were intentionally selected to make $\rho_i(\theta_i(t_0)) \approx 0 \quad \forall i = 1, 2$ to demonstrate the performance of the sub-task controller. The desired end-effector position $\xi_1(t)$, with ($\gamma = 1$) and without ($\gamma = 0$) user assistance is presented in Figs. 1(a) and 1(b), respectively. Figures 1(c) and 1(d) show the end-effector positions for the master and the slave systems, respectively. From Figs. 1(a) and 1(b), it can be clearly seen that the user assist mechanism provides great improvement to the desired end-effector position. It is worthwhile to mention that any desired trajectory can be converted into a velocity field; thus, user assist mechanism can always be used.[31] Figures 2(a) and 2(b) show the master system tracking error and coordination error, respectively. It can be easily inferred from these figures that the errors go to zero within few seconds enabling the master system to track the desired system accurately,

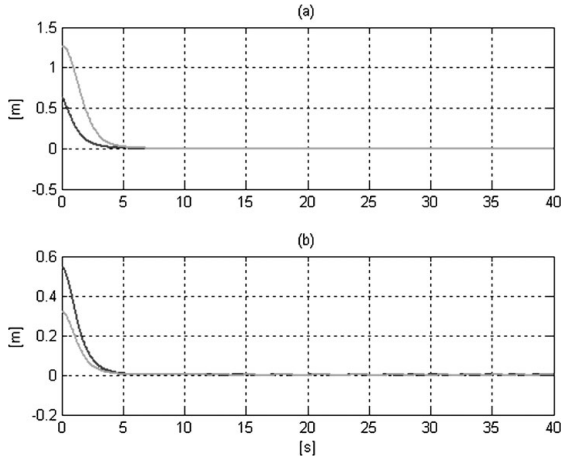


Fig. 2. Tracking errors (when $\gamma = 1$): (a) master system tracking error $e_1(t)$; (b) coordination error $e_2(t)$ between the master and the slave systems.

https://doi.org/10.1017/S026357470900544X Published online by Cambridge University Press

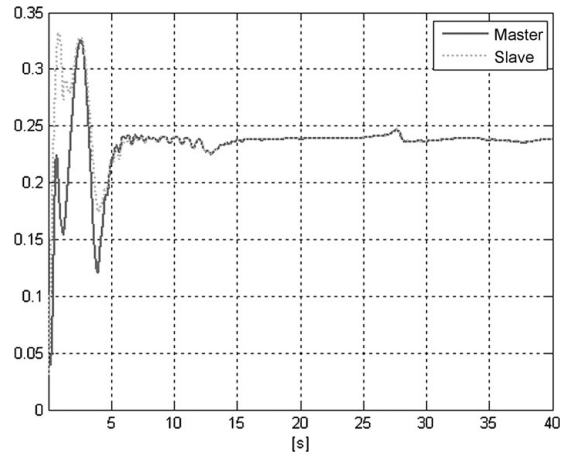


Fig. 3. Manipulability measure $\rho(\theta)$ for the master and the slave systems.

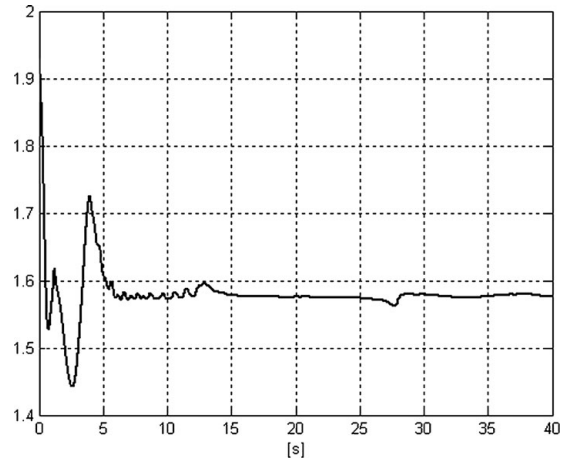


Fig. 4. Auxiliary positive function $y_a(t)$.

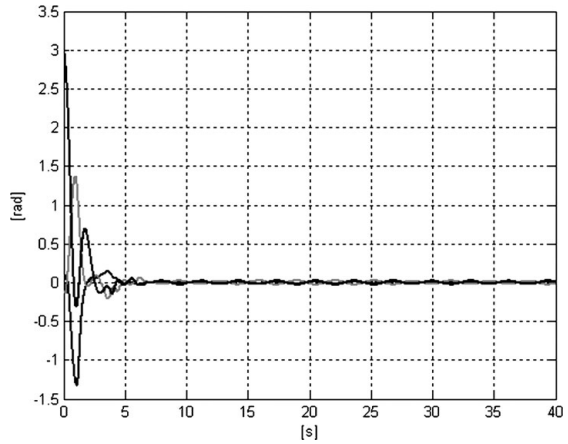


Fig. 5. Joint-space coordination error, $\tilde{\theta}_{ms} = \theta_m(t) - \theta_s(t)$, between the master and the slave systems (when $\gamma = 1$).

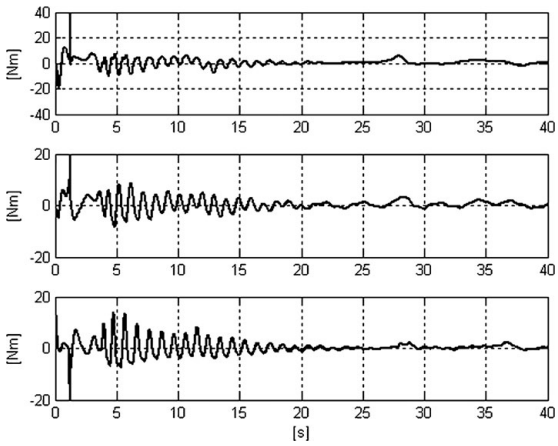


Fig. 6. Control input $T_1(t)$ for the master system (when $\gamma = 1$).

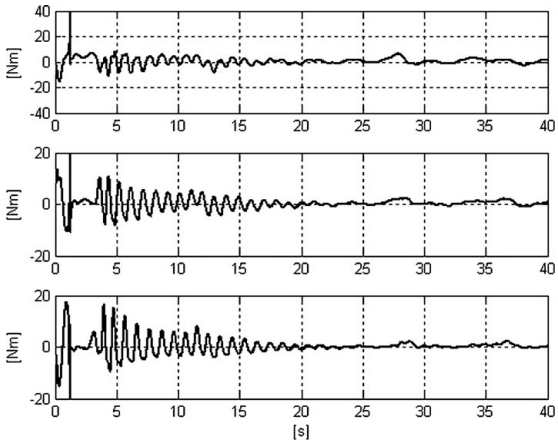


Fig. 7. Control input $T_2(t)$ for the slave system (when $\gamma = 1$).

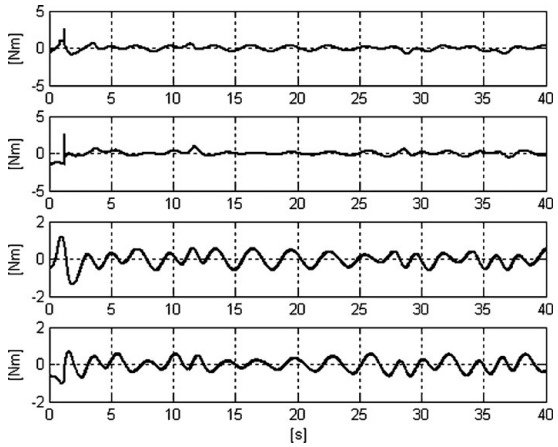


Fig. 8. The output of the nonlinear force observer $\hat{F}_T(t)$ for the task-space component of the unmeasurable force (when $\gamma = 1$).

and ensuring accurate coordination between the master and the slave systems. The sub-task controller's performance is demonstrated through the manipulability measure (i.e. $\rho_i(\cdot)$) in Fig. 3 where $\rho_i(\cdot) > 0 \quad \forall i = 1, 2$ for both the master and the slave systems; thus, avoiding the singular configurations even when the initial rest positions of both the systems were selected so as to have both the systems very close to their respective singular configurations. Figure 4 shows the measure of the positive auxiliary function $y_a(t)$. The joint-space coordination errors are shown in Fig. 5. The control inputs for the master and the slave systems are provided in Figs. 6 and 7, respectively. Figure 8 shows the observer designed to estimate the task-space component. Figures 9 and

https://doi.org/10.1017/S026357470900544X Published online by Cambridge University Press

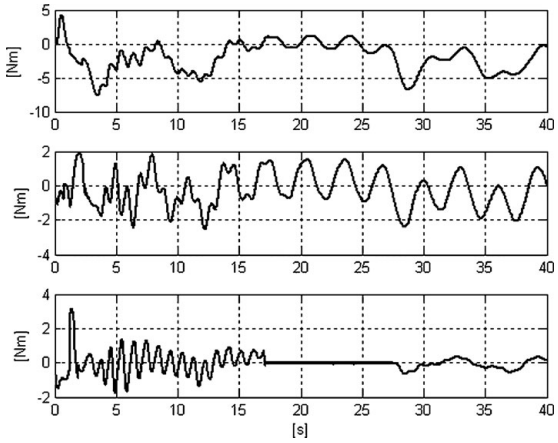


Fig. 9. The output of the nonlinear force observer $\hat{F}_H(t)$ for the unmeasurable user input force (when $\gamma = 1$).

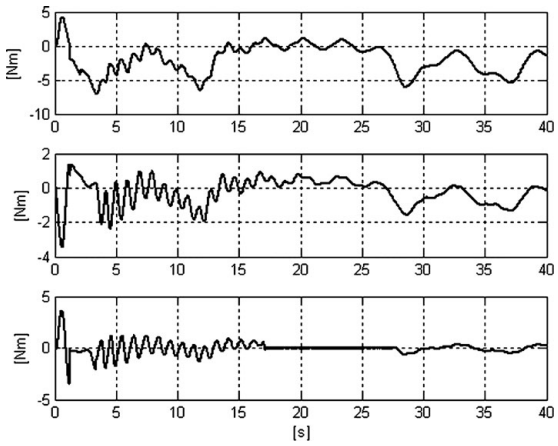


Fig. 10. The output of the nonlinear force observer $\hat{F}_E(t)$ for the unmeasurable environmental force (when $\gamma = 1$).

10 present the output of the nonlinear force observer for the unmeasurable user and environmental forces, respectively.

8. Conclusion

A controller for nonlinear teleoperator systems where both the master and the slave systems are kinematically redundant robot manipulators was presented. Lyapunov-based stability analysis was used to show that the proposed controller yields asymptotic results despite the unmeasurable user and environmental input forces. Also, the kinematic redundancy of the teleoperator system was utilized to integrate a sub-task controller. The proposed controller ensured that the master system accurately tracks a desired task-space trajectory, coordinates the master and the slave systems, and, additionally, satisfies sub-task objectives. An optional user assist mechanism was also presented that assists the user of the system to complete a predefined contour with the slave system. Numerical simulation results were presented to demonstrate the efficiency of the proposed task-space and sub-task-space controllers. Future work will focus on implementation of the proposed controller on real robot manipulators.

Acknowledgments

This work is supported in part by a DOE Contract and a Honda Corporation Grant.

Appendix A. Proof of Theorem 3

Proof. To facilitate the proof, a nonnegative function $V(t) \in \mathbb{R}$ is defined as follows:

$$V \triangleq \frac{1}{2}\dot{e}_N^T \dot{e}_N. \tag{A1}$$

The time derivative of (A1) is given as follows:

$$\dot{V} = \dot{e}_N^T[-(I_{2n} - J_f^+ J_f)(K_N \dot{e}_N - \hat{F}) + J_f^+ F_T - F - J_f^+ \dot{J}_f \dot{e}_N] \tag{A2}$$

where (76) was utilized. After utilizing the definition of $\dot{e}_N(t)$ given in (71) and the pseudo-inverse property given in (24), the transpose of $\dot{e}_N(t)$ can be written as follows:

$$\dot{e}_N^T = (g - \theta_f)^T (I_{2n} - J_f^+ J_f). \tag{A3}$$

After utilizing the property given in (23), the term $\dot{e}_N^T(I_{2n} - J_f^+ J_f)$, can be written as follows:

$$\dot{e}_N^T(I_{2n} - J_f^+ J_f) = (g - \theta_f)^T (I_{2n} - J_f^+ J_f) = \dot{e}_N^T \tag{A4}$$

where (A3) was utilized. Postmultiplying $\dot{e}_N^T(\cdot)$ by $J_f^+(\cdot)$ results in the following expression:

$$\dot{e}_N^T J_f^+ = (g - \theta_f)^T (I_{2n} - J_f^+ J_f) J_f^+. \tag{A5}$$

After utilizing the property given in (26), (A5) can be simplified as follows:

$$\dot{e}_N^T J_f^+ = 0_{1\times 2m}. \tag{A6}$$

After substituting (A4) and (A6) into (A2), the following simplified expression is obtained:

$$\dot{V} = -K_N \dot{e}_N^T \dot{e}_N + \dot{e}_N^T \tilde{F} \tag{A7}$$

where $\tilde{F}(t) \in \mathbb{R}^{2n}$ is defined as follows:

$$\tilde{F} \triangleq \hat{F} - F. \tag{A8}$$

The right-hand side of (A7) can be upper bounded as follows:

$$\dot{V} \leq -(K_N - \delta_1)\|\dot{e}_N\|^2 + \frac{1}{\delta_1}\|\tilde{F}\|^2 \tag{A9}$$

where the following inequality was utilized:

$$\|\dot{e}_N \tilde{F}\| \leq \delta_1 \|\dot{e}_N\|^2 + \frac{1}{\delta_1}\|\tilde{F}\|^2. \tag{A10}$$

https://doi.org/10.1017/S026357470900544X Published online by Cambridge University Press

After integrating (A9), the following expression is obtained:

$$\int_{t_0}^{\infty} \dot{V}_3(\tau)\,\mathrm{d}\tau \le -\varepsilon \int_{t_0}^{\infty} \|\dot{e}_N(\tau)\|^2\,\mathrm{d}\tau + \frac{1}{\delta_1}\int_{t_0}^{\infty} \|\tilde{F}(\tau)\|^2\,\mathrm{d}\tau \qquad \text{(A11)}$$

where $\varepsilon \triangleq K_N - \delta_1 \in \mathbb{R}$. The expression given in (A11) can be rearranged as follows:

$$\varepsilon \int_{t_0}^{\infty} \|\dot{e}_N(\tau)\|^2\,\mathrm{d}\tau \le \frac{1}{\delta_1}\int_{t_0}^{\infty} \|\tilde{F}(\tau)\|^2\,\mathrm{d}\tau + V(t_0) - V(\infty). \qquad \text{(A12)}$$

Since $V(\infty)$ is nonnegative, the expression in (A12) can be rewritten as follows:

$$\varepsilon \int_{t_0}^{\infty} \|\dot{e}_N(\tau)\|^2\,\mathrm{d}\tau \le \frac{1}{\delta_1}\int_{t_0}^{\infty} \|\tilde{F}(\tau)\|^2\,\mathrm{d}\tau + V(t_0). \qquad \text{(A13)}$$

After utilizing the fact that $\tilde{F}(t) \in \mathcal{L}_2$, the following expression can be obtained*:

$$\int_{t_0}^{\infty} \|\tilde{F}(\tau)\|^2\,\mathrm{d}\tau \le \delta_2. \qquad \text{(A14)}$$

After utilizing (A14), the expression given in (A13) can be written as follows:

$$\varepsilon \int_{t_0}^{\infty} \|\dot{e}_N(\tau)\|^2\,\mathrm{d}\tau \le \left(\frac{\delta_2}{\delta_1} + V(t_0)\right). \qquad \text{(A15)}$$

From (A15), it is clear that $\dot{e}_N(t) \in \mathcal{L}_2$. From the result of Theorem 3, it can be seen that $g(t)$, $\dot{g}(t) \in \mathcal{L}_\infty$. Further, it is clear from the result of Theorem 1 that $\theta_f(t) \in \mathcal{L}_\infty$ and from the result of Theorem 2 that $J_f(\cdot)$, $J_f^+(\cdot) \in \mathcal{L}_\infty$ therefore from (71), $\dot{e}_N(t) \in \mathcal{L}_\infty$. As seen from the result of Theorem 1, $\hat{F}(t) \in \mathcal{L}_\infty$. It is clear from (75) that $u_N(t) \in \mathcal{L}_\infty$, therefore it can be easily concluded from (76) that $\ddot{e}_N(t) \in \mathcal{L}_\infty$. The facts that $\dot{e}_N(t) \in \mathcal{L}_2 \cap \mathcal{L}_\infty$ and $\ddot{e}_N(t) \in \mathcal{L}_\infty$ can be utilized along with Barbalat's Lemma[13] to prove that

$$\|\dot{e}_N(t)\| \to 0 \quad \text{as} \quad t \to \infty. \qquad \text{(A16)}$$

Appendix B. Proof of pseudo-inverse property given in (27)

The following expression can be obtained for (27):

$$(I_{2n} - J_f^+ J_f)J_\phi = \dot{J}_f^+ J_f + J_f^+ \dot{J}_f J_f^+ J_f - J_f^+(J_f \dot{J}_f^+ + J_f J_f^+ \dot{J}_f J_f^+)J_f \qquad \text{(B1)}$$

* From the proof of Theorem 1, it is clear that $\dot{\tilde{\theta}}_f(t) \in \mathcal{L}_2$. Then, from (34) and (A8), it can be concluded that $\tilde{F}(t) \in \mathcal{L}_2$.

where (28) was utilized. After utilizing the pseudo-inverse property given in (21), the term $J_f J_f^+ \dot{J}_f J_f^+$ on the right-hand side of (B1), can be written as follows:

$$J_f J_f^+ \dot{J}_f J_f^+ = \dot{J}_f J_f^+. \qquad \text{(B2)}$$

Substituting (B2) into (B1), results in the following expression:

$$(I_{2n} - J_f^+ J_f)J_\phi = \dot{J}_f^+ J_f + J_f^+ \dot{J}_f J_f^+ J_f - J_f^+(J_f \dot{J}_f^+ + \dot{J}_f J_f^+)J_f. \qquad \text{(B3)}$$

The expression in (B3) can be rewritten in a simplified form as follows:

$$(I_{2n} - J_f^+ J_f)J_\phi = \dot{J}_f^+ J_f + J_f^+ \dot{J}_f J_f^+ J_f - J_f^+ \frac{\mathrm{d}}{\mathrm{d}t}(J_f J_f^+)J_f. \qquad \text{(B4)}$$

Utilizing the pseudo-inverse property given in (21), results in the following expression

$$(I_{2n} - J_f^+ J_f)J_\phi = \dot{J}_f^+ J_f + J_f^+ \dot{J}_f J_f^+ J_f = J_\phi \qquad \text{(B5)}$$

where (28) was utilized.

References

1. N. Nath, E. Tatlicioglu and D. M. Dawson, "Teleoperation with Kinematically Redundant Robot Manipulators with Sub-Task Objectives," *Proceedings of IEEE International Conference on Decision and Control*, Cancun, Mexico (Dec. 2008) pp. 4320–4325.
2. T. B. Sheridan, "Teleoperation, telerobotics and telepresence: A progress report," *Control Eng. Prac.* **3**(2), 205–214 (1995).
3. P. Berkelman and J. Ma, "A Compact, Modular, Teleoperated Minimally Invasive Surgery System," *Proceedings of IEEE/RAS-EMBS International Conference on Biomedical, Robotics and Biomechatronics*, Pisa, Italy (Feb. 2006) pp. 702–707.
4. F. Ogaki and K. Suzuki, "Adaptive Teleoperation of a Mobile Robot Under Communication Time Delay," *IEEE International Workshop on ROSE*, Ottawa, Canada (Oct. 2007) pp. 1–6.
5. E. Slawinski, J. Postigo and V. Mutt, "Stable Teleoperation of Mobile Robots," *Proceedings of IEEE International Conference on Mechatronics and Automation*, Luoyang, China (Jun. 2006) pp. 318–323.
6. D. A. Lawrence, "Stability and transparency in bilateral teleoperation," *IEEE Trans. Robot. Automat.* **9**(5), 624–637 (1993).
7. P. F. Hokayem and M. W. Spong, "Bilateral teleoperation: An historical survey," *Automatica* **42**(12), 2035–2057 (2006).
8. G. S. Chirikjian and J. W. Burdick, "Hyper-Redundant Robot Mechanisms and Their Applications," *Proceedings of IEEE/RSJ International Conference on Intelligent Robots Systems*, Osaka, Japan (Nov. 1991) pp. 185–190.
9. Y. Nakamura, *Advanced Robotics Redundancy and Optimization* (Addison-Wesley, Reading, MA, 1991).
10. D. N. Nenchev, "Redundancy resolution through local optimization: A reveiw," *J. Rob. Syst.* **6**(6), 769–798 (1993).
11. B. Siciliano, "Kinematic control of redundant robot manipulators: A tutorial," *J. Intell. Rob. Syst.* **3**, 201–212 (1990).

https://doi.org/10.1017/S026357470900544X Published online by Cambridge University Press

12. E. Tatlicioglu, *Control of Nonlinear Mechatronic Systems* (VDM Verlag Dr. Mueller e.K., Germany, 2008).
13. W. E. Dixon, A. Behal, D. M. Dawson and S. Nagarkatti, *Nonlinear Control of Engineering Systems: A Lyapunov-Based Approach* (Birkhauser, Boston, MA, 2003).
14. E. Zergeroglu, D. Dawson, I. Walker and A. Behal, "Nonlinear Tracking Control of Kinematically Redundant Robot Manipulators," *Proceedings of American Control Conference*, Chicago, IL (Jun. 2000) pp. 2513–2517.
15. R. Colbaugh and K. Glass, "Robust adaptive control of redundant manipulators," *J. Intell. Rob. Syst.* **14**(1), 68–88 (1995).
16. O. Khatib, "Dynamic Control of Manipulators in Operational Space," *IFTOMM Congress Theory of Machines and Mechanisms*, New Delhi, India (1983) pp. 1–10.
17. J. Yuan, "A general photogrammetric method for determining object position and orientation," *IEEE Trans. Robot. Autom.* **5**(2), 129–142 (1989).
18. D. Hwang and B. Hannaford, "Teleoperation performance with a kinematically redundant slave robot," *Int. J. Rob. Res.* **17**, 579–597 (1998).
19. H. Das, T. B. Sheridan and J. J. E. Slotine, "Kinematic Control and Visual Display of Redundant Teleoperators," *IEEE International Conference on System, Man, and Cybernetics,* Cambridge, MA (Nov. 1989) pp. 1072–1077.
20. E. Tatlicioglu, M. McIntyre, D. M. Dawson and T. Burg, "Coordination Control for Haptic and Teleoperator Systems," *Proceedings of IEEE International Conference on Decision and Control*, San Diego, CA (Dec. 2006) pp. 2937–2942.
21. F. Lewis, D. Dawson and C. Abdallah, *Robot Manipulator Control: Theory and Practice* (Marcel Dekker, Inc., New York, NY, 2004).
22. D. Lee and P. Y. Li, "Passive Coordination of Nonlinear Bilateral Teleoperated Manipulators," *Proceedings of IEEE International Conference on Robotics and Automation*, Washington DC (May 2002) pp. 3278–3283.
23. D. Lee and P. Y. Li, "Passive bilateral feedforward control of linear dynamically similar teleoperated manipulators," *IEEE Trans. Robot. Autom.* **19**(3) 443–456 (2003).
24. E. Zergeroglu, D. M. Dawson, I. Walker and A. Behal, "Nonlinear Tracking Control of Kinematically Redundant Robot Manipulators," *Proceedings of American Control Conference*, Chicago, IL (Jun. 2000) pp. 2513–2517.
25. E. Tatlicioglu, D. Braganza, T. Burg and D. Dawson, "Adaptive control of redundant robot manipulators with sub-task extensions," *Robotica* (to appear) (doi: 10.1017/S0263574708005274).
26. E. Tatlicioglu, M. McIntyre, D. Dawson and I. Walker, "Adaptive nonlinear tracking control of kinematically redundant robot manipulators," *Int. J. Rob. Automat.* **23**(2), 98–105 (2008).
27. H. T. Sahin, U. Ozbay and E. Zergeroglu, "Quaternion Based Robust Tracking Control of Kinematically Redundant Manipulators Subject to Multiple Self-Motion Criteria," *Proceedings of IEEE International Conference on Decision and Control*, San Diego, CA (Dec. 2006) pp. 6462–6467.
28. E. Zergeroglu, H. T. Sahin, U. Ozbay and U. A. Tektas, "Robust Tracking Control of Kinematically Redundant Robot Manipulators Subject to Multiple Self-Motion Criteria," *Proceedings of IEEE International Conference on Control Applications*, Munich, Germany (Oct. 2006) pp. 2860–2865.
29. D. Braganza, M. L. McIntyre, D. M. Dawson and I. D. Walker, "Whole Arm Grasping Control for Redundant Robot Manipulators," *Proceedings of American Control Conference*, Minneapolis, MN (Jun. 2006) pp. 3194–3199.
30. Y. Oh, W. K. Chung and Y. Youm, "Extended Impedance Control of Redundant Manipulators Using Joint Space Decomposition," *Proceedings of IEEE International Conference on Robotics Automation*, Albuquerque, NM (Apr. 1997) pp. 1080–1087.
31. P. Li and R. Horowitz, "Passive velocity field control of mechanical manipulators," *IEEE Trans. Robot. Automat.* **15**(4), 751–763 (1999).
32. P. Hsu, J. Hauser and S. Sastry, "Dynamic control of redundant robot manipulators," *J. Rob. Syst.* **6**(3), 133–148 (1989).
33. M. W. Spong and M. Vidyasagar, *Robot Dynamics and Control* (John Wiley and Sons, New York, NY, 1989).
34. I. Cervantes, R. Kelly, J. Alvarez-Ramirez and J. Moreno, "A robust velocity field control," *IEEE Trans. Contr. Syst. Technol.* **10**(6), 888–894 (2002).
35. J. J. Craig, *Introduction to Robotics: Mechanics and Control*, 3rd ed. (Prentice Hall, New York, NY, 2004).

https://doi.org/10.1017/S026357470900544X Published online by Cambridge University Press